JOINT INSTITUTE FOR NUCLEAR RESEARCH
Veksler and Baldin laboratory of High Energy Physics

FINAL REPORT ON THE INTEREST PROGRAMME

Soft Photon study in hadron and nuclear interactions

Supervisor:
Prof Elena Kokoulina

Student:
Alexandra-Gabriela Şerban
Faculty of Physics, University of Bucharest

Participation period:
November 02 - December 11, Wave 2

Dubna, 2020

Contents

Introduction

For over 30 years there has been no comprehensive understanding of the mechanism of soft photons formation. Soft photons (SPh) are the direct products of high energy interactions. They are not decay products of secondary particles and their energy is smaller than 50 MeV.

Experimental data indicate an excess of their yield in hadron and nuclear interactions. The existing theoretical calculations based on the quantum electrodynamics can not predict and explain this excess. For a more thorough study of this phenomenon the building of the future accelerator complex NICA makes possible to carry out such studies in different interactions.

Up to now the nature of SPh remains enigmatic. Apparently, they are formed in the region of non perturbative quantum chromodynamics and physicists build phenomenological models. The most successful model is based on the hypothesis of the cold quark-gluon plasma (QGP) formation. This model implies the formation of a quark-gluon system which consists of a few quarks, antiquarks and gluons (about 40 partons). These partons are encountering each other and reradiate soft photons because they do not have enough energy to produce hadrons, the main reactions being Compton scattering and pair annihilation.

Project goals

- Getting accustomed to Geant4 packet and CERN Root open-source data analysis framework

- Data taking and data processing for different simulations

- Study of the operation of electromagnetic calorimeters of homogeneous (crystalline) and heterogeneous ('shashlyk' and 'spaghetti') types

Interaction of radiation with matter

Particles can be detected only through their interactions with matter. There are specific interactions for charged particles which are different from those of neutral particles, such as photons. Every interaction process can be used as a basis for a detector concept. The main interactions of charged particles with matter are ionisation and excitation. For relativistic particles, bremsstrahlung - if the charged particles are decelerated in the Coulomb field of the nucleus, a fraction of their kinetic energy will be emitted in form of photons - energy losses must also be considered. Neutral particles must produce charged particles in an interaction that are then detected via their characteristic interaction processes. In the case of photons, these processes are the photoelectric effect, Compton scattering and pair production of electrons. The electrons produced in these photon interactions can be observed through their ionisation in the sensitive volume of the detector.

1. Radiation length (X_0)

It is a characteristic of a material related to the energy loss of high energy particles electromagnetically interacting with it.

$$X_0 = \frac{716.4 \cdot A[\mathrm{g/mol}]}{Z(Z+1)\ln\dfrac{287}{\sqrt{Z}}} \quad \mathrm{g/cm^2} \tag{1}$$

The radiation length for a mixture of elements or a compound can be approximated by,

$$X_0 = \frac{1}{\displaystyle\sum_{i=1}^{N} \frac{f_i}{X_0^i}} \tag{2}$$

where f_i are the mass fractions of the components with the radiation length X_0^i.

The mass fraction can be calculated using the following formula,

$$f_i = \frac{A_i v_i}{\sum_{i=1}^{N} A_k v_k} \tag{3}$$

where,

A = atomic mass in g/mole
v = valence

In order to obtain the radiation length expressed in cm we have to divide it by the density ρ of the considered material.

2. Critical energy (E_c)

Energy losses due to bremsstrahlung are proportional to the energy while ionisation energy losses beyond the minimum of ionisation are proportional to the logarithm of the energy. The energy, where these two interaction processes for electrons lead to equal energy losses, is called the critical energy E_c.

$$E_\mathrm{c} = \frac{610 \text{ MeV}}{Z + 1.24} \tag{4}$$

In the case of compound systems, the critical energy can be calculated using the following formula,

$$E_\mathrm{c} = \frac{550 \text{ MeV}}{Z_{eff}} \tag{5}$$

where Z_{eff} is given by,

$$Z_{eff} = \frac{\sum_{i=1}^{N} Z_i f_i}{\sum_{i=1}^{N} f_i} \tag{6}$$

3. Molière radius (R_M)

The lateral width of an electromagnetic cascade is mainly determined by multiple scattering and can be best characterised by the Molière radius.

$$R_{\mathrm{M}} = \frac{21 \text{ MeV}}{E_{\mathrm{c}}} X_0 \quad \mathrm{g/cm^2} \tag{7}$$

Calorimetry

Calorimetric methods imply total absorption of the particle energy in a bulk of material followed by the measurement of the deposited energy. High-energy photons, electrons and hadrons can interact with media producing secondary particles which leads to a shower development. Then the particle energy is deposited in the material much more efficiently. Thus calorimeters are most widely used in high energy physics to detect the electromagnetic and hadronic showers. Accordingly, such detector systems are referred to as electromagnetic and hadron calorimeters.

1. Electromagnetic calorimeters

The dominating interaction processes for spectroscopy in the MeV energy range are the photoelectric and Compton effect for photons and ionisation and excitation for charged particles. At high energies, electrons lose their energy almost exclusively by bremsstrahlung while photons lose their energy by electron–positron pair production. The most important properties of electron cascades can be understood using a simplified model. Let E_0 be the energy of a photon incident on a bulk material. After one radiation length the photon produces an e^+ e^- pair; electrons and positrons emit after another radiation length one bremsstrahlung photon each, which again are transformed into electron–positron pairs. When the particle energy falls below the critical value E_c, absorption processes like ionisation for electrons and Compton and photoelectric effects for photons start to dominate. At this step of multiplication, the position of the shower maximum is reached.

This very simple model describes correctly the most important qualitative characteristics of electromagnetic cascades:

a) To absorb most of the energy of the incident photon the total calorimeter thickness should be more than 10 – 15 X_0

b) The position of the shower maximum increases slowly with energy. Thus, the thickness of the calorimeter should increase as the logarithm of the energy

c) The energy leakage is caused mostly by soft photons escaping the calorimeter at the sides (lateral leakage) or at the back (rear leakage)

In reality the shower development is much more complicated, an accurate description of the shower development being a difficult task. However, due to the increase of the computer capacity, an accurate description is obtained from Monte Carlo simulations.

A. Homogeneous calorimeters

Homogeneous calorimeters are constructed from a material combining the properties of an absorber and a detector. It means that practically the total volume of the calorimeter is sensitive to the deposited energy. These calorimeters are based on the measurement of the scintillation light (scintillation crystals, liquid noble gases), ionisation (liquid noble gases) and the Cherenkov light (lead glass or heavy transparent crystals).

The main parameters of electromagnetic calorimeters are the energy and position resolution for photons and electrons. The energy resolution $\frac{\sigma_E}{E}$ is determined both by physical factors like the fluctuation of the energy leakage or photoelectron statistics and technical ones like nonuniformity of crystals.

B. Sampling calorimeters

A sampling calorimeter is a calorimeter designed as an array of thin counters separated by layers of absorbers and only a sample of the energy deposition is measured. As sensitive elements of sampling calorimeters are used: gas-filled chambers, liquid-argon ionisation detectors, 'warm' liquids and scintillators.

A normal sampling calorimeter of absorber plates and scintillator sheets can also be read out by wavelength-shifter rods or fibres running through the scintillator plates perpendicularly. The technique of wavelength-shifter readout allows to build rather compact calorimeters. The scintillation counters used in calorimeters must not necessarily have the form of plates alternating with absorber layers, they can also be embedded as scintillating fibres. They can either be read out directly or via light-guide fibres by photomultipliers (spaghetti calorimeter). This type of calorimeter provides both high energy resolution and precise timing for photons due to the short decay time of the light flash of the plastic scintillator. Even a better energy resolution was reported for a 'shashlik ' - type sampling calorimeter developed for the KOPIO experiment.

2. Hadron calorimeters

Hadron calorimeters work along the same lines as electron – photon calorimeters, the main difference being that for hadron calorimeters the longitudinal development is determined by the average nuclear interaction length λ_I which is much larger than the radiation length X_0 describing the behaviour of electron–photon cascades. This implies that hadron calorimeters have to be much larger than electromagnetic shower counters. Frequently, electron and hadron calorimeters are integrated in a single detector.

Apart from the larger longitudinal development of hadron cascades, their lateral width is also sizably increased compared to electron cascades. While the lateral structure of electron showers is mainly determined by multiple scattering, in hadron cascades it is caused by large transverse momentum transfers in nuclear interactions.

In contrast to electrons and photons, whose electromagnetic energy is almost completely recorded in the detector, a substantial fraction of the energy in hadron cascades remains invisible. This is related to the fact that some part of the hadron energy is used to break up nuclear bonds. This nuclear binding energy is provided by the primary and secondary hadrons and does not contribute to the visible energy. Furthermore, extremely short-range nuclear fragments are produced in the break-up of nuclear bonds. In sampling calorimeters, these fragments do not contribute to the signal since they are absorbed before reaching the detection layers.

Geant4 Simulations

A. BGO crystal

BGO ($Bi_4Ge_3O_{12}$) is a high Z, high density scintillation material. Due to the high atomic number of Bismuth and the material's high density, BGO is a very efficient gamma ray absorber.

Element	Z	A (g/mole)	v	f	X_0 (g/cm^2)	ρ (g/cm^3)	$\tilde{X}_0$ (cm)
O	8	16	12	0.154	34.461	1.141	30.202
Ge	32	72.63	3	0.175	12.550	5.323	2.358
Bi	83	208.98	4	0.671	6.220	9.747	0.638

Table 1: Properties of the component elements of BGO crystal

The mass fraction was calculated using formula 3 and the radiation length using formula 1.

The composite density of the BGO crystal is calculated using the denisties and mass fractions of the component elements and it is given by,

$$\rho^{BGO} = 7.647 \ \text{g/cm}^3 \tag{8}$$

In order to obtain the radiation length for the BGO crystal we employ formula 2 and obtain,

$$X_0^{BGO} = 0.884 \text{ cm} \tag{9}$$

The next step is to calculate the critical energy for the BGO crystal. Making use of the formulas 5 and 6, we get,

$$E_c^{BGO} = 8.796 \text{ MeV} \tag{10}$$

The Molière radius is computed using formula 7 and it has the following value,

$$R_M^{BGO} = 2.111 \text{ cm} \tag{11}$$

All the above calculations were used in simulating a homogeneous calorimeter based on a BGO crystal using Geant4.

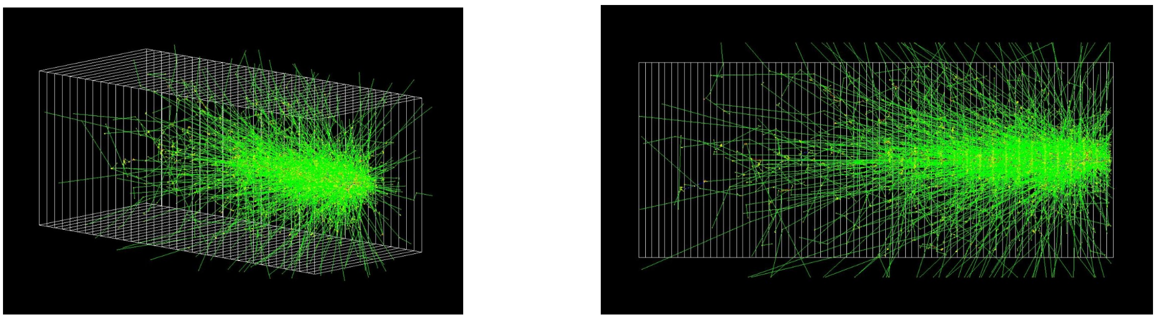

Figure 1: Electromagnetic shower in BGO crystal

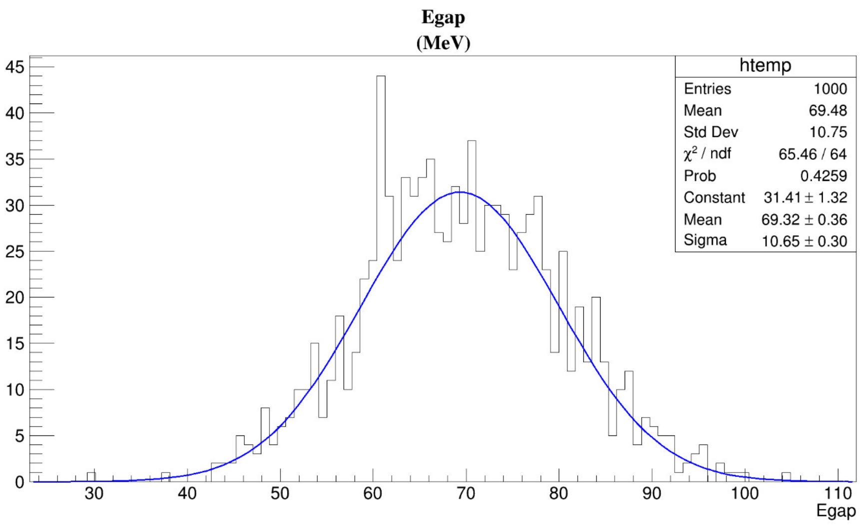

Figure 2: Energy release in the BGO crystal for incoming photons having the energy 150 MeV

The energy resolution for the BGO crystal is given by,

$$\left(\frac{\sigma_E}{E}\right)_{BGO} = 7.1\,\% \tag{12}$$

B. Fe/liquid Xe calorimeter

Xenon is a colorless and dense noble gas, while Iron is a metal which belongs to the first transition series and group 8 of the periodic table.

Element	Z	A (g/mole)	ρ (g/cm^3)
Fe	26	55.845	7.874
Xe	54	131.294	2.942

Table 2: Properties of Fe and Xe

For the liquid Xe we calculate the radiation length using formula 1 and obtain,

$$X_0^{Xe} = 2.937 \text{ cm} \tag{13}$$

The next step is to calculate the critical energy for the liquid Xe using formula 4,

$$E_c^{Xe} = 11.043 \text{ MeV} \tag{14}$$

The Molière radius is computed making use of formula 7,

$$R_M^{Xe} = 5.587 \text{ cm} \tag{15}$$

The calculations were used in simulating a sampling calorimeter based on Fe as an absorber and on liquid Xe as the detection material using Geant4.

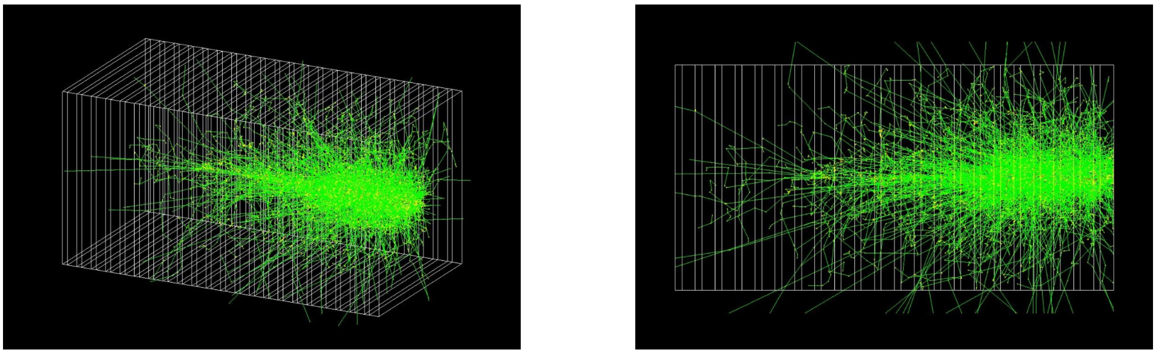

Figure 3: Electromagnetic shower in the sampling calorimeter made of Fe and liquid Xe

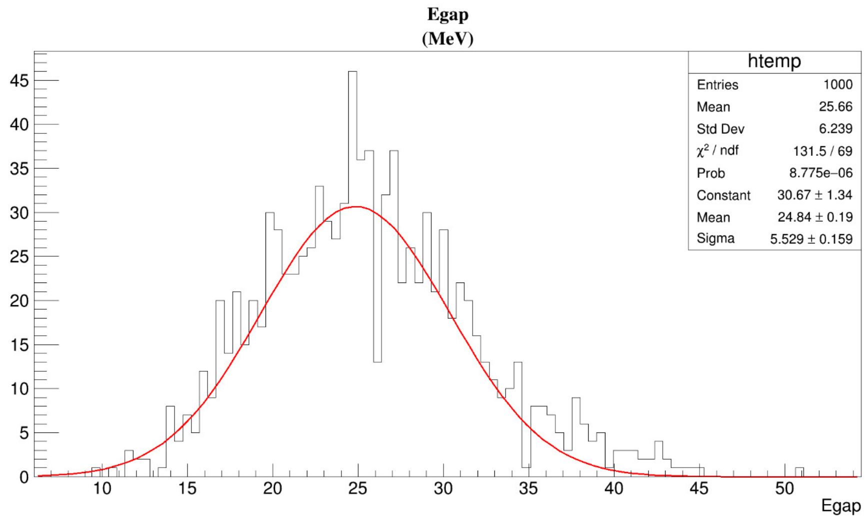

Figure 4: Energy release in the sampling calorimeter made of Fe and liquid Xe crystal for incoming photons having the energy 150 MeV

The energy resolution for the Fe/liquid Xe sampling calorimeter has the following value,

$$\left(\frac{\sigma_E}{E}\right)_{Fe/liquid\,Xe} = 3.7\,\% \tag{16}$$

C. GaGG 'shashlik' calorimeter

The studied 'shashlik' calorimeter is a heterogeneous one for which we have chosen a mono-crystal of Gadolinium-Gallium Garnet, $Gd_3Al_2Ga_3O_{12}$ (GaGG), as a scintillator and Tungsten + Copper composite as the absorber material. GaGG is a fast-acting scintillator which demonstrates good radiation resistance.

Element	Z	A (g/mole)	v	f	X_0 (g/cm^2)	ρ (g/cm^3)	$\tilde{X}_0$ (cm)
Gd	64	157.250	3	0.508964	7.564	7.4	1.022
Al	13	26.982	2	0.058221	24.265	2.7	8.987
Ga	31	69.723	3	0.225669	12.772	6.095	2.095
O	8	16	12	0.207146	34.461	1.141	30.202

Table 3: Properties of the component elements of the GaGG 'shashlik' ECal

The composite density is given by,

$$\rho^{GaGG} = 5.535 \ \text{g/cm}^3 \tag{17}$$

The radiation length for GaGG is,

$$X_0^{GaGG} = 1.615 \text{ cm} \tag{18}$$

The critical energy has the value,

$$E_c^{GaGG} = 1.351 \text{ MeV} \tag{19}$$

and the Molière radius is,

$$R_M^{GaGG} = 25.1 \text{ MeV} \tag{20}$$

We consider that the absorber is made of 50 % W and 50 % Cu.

Element	Z	A (g/mole)	ρ (g/cm^3)	X_0 cm
W	74	183.84	19.30	0.35
Cu	29	63.55	9.96	1.44

Table 4: Properties of W and Cu

The radiation length for the W/Cu composite is given by,

$$X_0^{W/Cu} = 0.563 \text{ cm} \tag{21}$$

and the density is,

$$\rho^{W/Cu} = 11.187 \text{ g/cm}^3 \tag{22}$$

Figure 5: Electromagnetic shower in GaGG 'shashlik' ECal

The energy resolution for the GaGG 'shashlik' ECal is given by,

$$\left(\frac{\sigma_E}{E}\right)_{GaGG} = 5.6\ \% \tag{23}$$

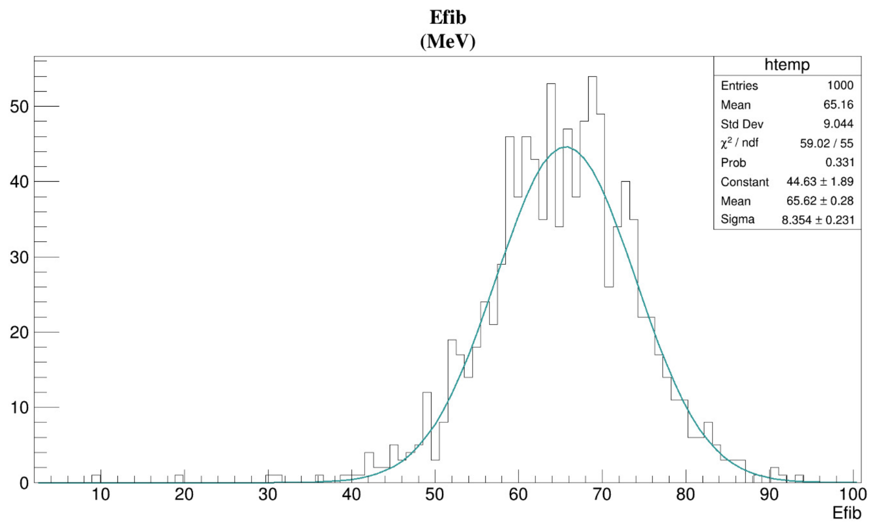

Figure 6: Energy release in the GaGG 'shashlik' ECal for incoming photons having the energy 150 MeV

Conclusions

In our study we constructed three different types of calorimeteres: a homogeneous one based on a BGO crystal, a sampling calorimeter having as a detector material liquid Xenon and as an absorber Fe and a heterogeneous 'shashlik' ECal made of GaGG. By calculating different parameters, such as: radiation length, critical energy and Molière radius, we were able to establish the dimensions of the calorimeters in the z direction on which the photons are sent and on the transverse direction.

After performing various simulations in Geant4, the obtained histograms were analyzed using CERN Root. We calculated for each calorimeter the energy resolution in the case of 150 MeV photons coming in the z direction. We saw that the best energy resolution is obtained in the BGO crystal. However, crystal ECals are very expensive. We observed that we lose a little with the energy resolution in the case of the GaGG 'shashlik' ECal, but we gain with the cost of production which is much lower.

Our main task was to make simulations of different calorimeters and to find the optimal construction for registering soft photons. Thus, the 'shashlik' calorimeter with GaGG as a scintillator and W/Cu as an absorber is a good choice in the study of soft photons since it has a good energy resolution compared to a crystalline calorimeter, but it is more advantageous when we consider the price we need to pay for building the calorimeters. Thus, it can be used in future experimental studies of photon beams at the Nuclotron facility in JINR.

Bibliography

[1] P. Lichard, L. Van Hove, The cold quark-gluon plasma as a source of very soft photons in high energy collisions, Physics Letters B245, 605-608 (1990)

[2] Elena Kokoulina, Nurlan Barlykov, Vladimir Dudin, Andrey Kutov, Vladimir Nikitin, Vasilii Riadovikov, Roman Shulyakovsky, Study of soft photon yield in pp and AA interactions at JINR, The European Physical Journal Conferences 235:03003 (2020)

[3] Claus Grupen, Boris Shwartz. *Particle Detectors,* 2^{nd} *edition.* Cambridge University Press, 2008.

[4] David Cockerill. *Introduction to Calorimeters.* Southampton Lecture, 4 May 2016.

[5] Christophe Ochando. *Lectures on calorimetry.* ESIPAP 2017.

[6] https://pdg.lbl.gov/2020/AtomicNuclearProperties/index.html

Acknowledgments

I am thankful to Professor Elena Kokoulina who guided my steps in the understanding of calorimetry simulations using Geant4 and of analysis using CERN Root.